

$$\begin{aligned}
P_{PV} &= \eta_{MPP} I_t A \\
&= \frac{\eta_{MPP}(I_t, T_m)}{\eta_{STC}} \frac{I_t}{1000W/m^2} P_{inst}
\end{aligned} \tag{5}$$

The P_{PV} power computed in Eqn. 5 represents the DC power output. The parameter A in Eqn. 5 is the surface area of the module, P_{inst} is the PV installed capacity and η_{STC} is the module efficiency under standard test conditions (STC). The standard test conditions are defined by module temperature of $25^\circ C$, incoming irradiance of $1000 W/m^2$ and the standard spectrum of air mass AM1.5. We have used the DC to AC power conversion model by [20] which includes the inverter efficiency and inverter losses. The final AC power output for each model grid point is upscaled to prepare the country level PV power time-series.

2.3.3. CSP power model

Power output from CSP plants depends on solar irradiance levels (duration and intensity), solar field size and system efficiencies. We have adopted a parametric model to compute CSP power. This model (Solar Advisor Model (SAM)) was developed by NREL, in conjunction with Sandia National Laboratory and in partnership with the U.S. Department of Energy [22]. The functional form of the model is given in Eqn. 6. The explanation of the different quantities used in Eqn. 6 is summarised in Table 3. The net power output P_{CSP} estimated in Eqn. 6 represents the gross power output excluding the share required to operate the power plant. This includes fuel handling equipment, water pumps, combustion and cooling air fans, pollution control equipment, and other electricity needs. The unit of P_{CSP} used here is MW. The final CSP power is computed by multiplying the net power with plant's installed capacity.

$$P_{CSP} = (1 - Loss_{parasitic}) \cdot \eta_{Turbine} \cdot A_{sf} \cdot (DNI \cdot \eta_{opt} - Loss_{HCE} - Loss_{SFP}) \tag{6}$$

Variable	Meaning (unit)	Value
$Loss_{parasitic}$	Electric parasitic loss	0.111 [13]
$\eta_{Turbine}$	Design turbine gross efficiency	0.364 [13]
A_{sf}	Solar Field Area (m^2)	685,666 [24]
η_{opt}	Optical efficiency	0.602 [13]
$Loss_{HCE}$	HCE Thermal Losses (W/m^2)	42.629 [22]
$Loss_{SFP}$	Solar Field Piping Heat Losses (W/m^2)	10.05 [22]

Table 3: List of variables related to CSP power calculation

2.3.4. Hydro power model

Inflow into hydro dams is calculated via runoff data from ERA Interim. A simple potential energy approach is chosen. The potential gravitational energy relative to the sea level is given by

$$U = mgh,$$

where m is the mass, $g = 9.81\text{m/s}^2$ the constant of gravitational acceleration on Earth and h the height above sea level. For the calculation of inflow into storages, that formula is applied,

$$U = fmgh.$$

f a the normalization constant that ensures $\langle \text{Inflow}_n \rangle = \langle G_n^H \rangle$, where G_n^H is today's generation from hydro in the corresponding country. The mass is calculated from the runoff data. The potential energy calculated from this approach is then assumed to be the inflow into the hydro storage of a country. Fig. 10 shows the daily sum of the inflows into hydro storages for all investigated countries for the years 2003-2004. A strong seasonal pattern with high rates of inflow especially in Spring can be observed.

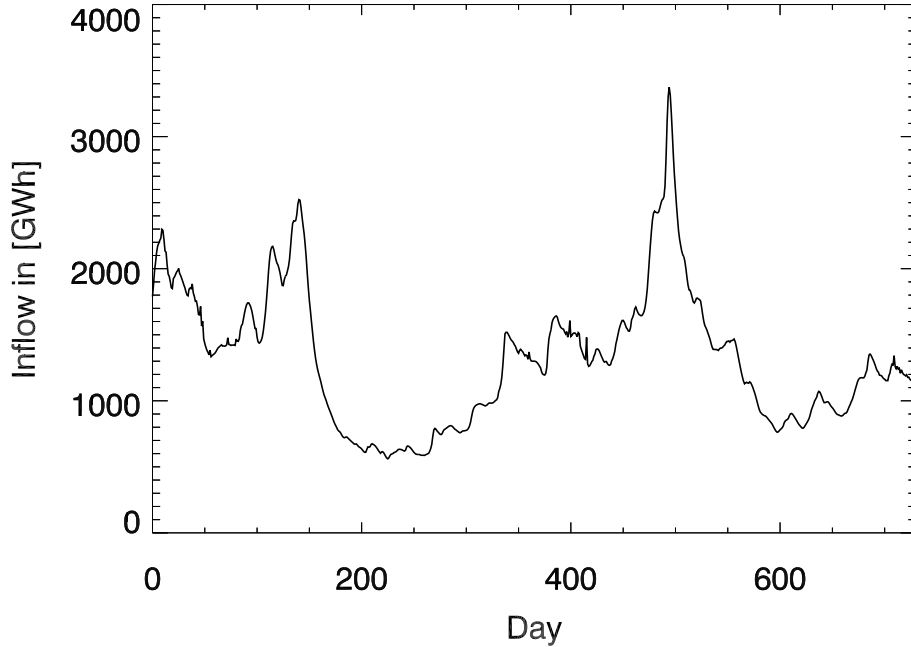


Figure 10: Daily hydro inflow for the whole investigated regions for the years 2002-2003.

3. Analysis and Discussion

The long-term time-series of different technologies are thoroughly analysed and validated. This section summarises validation and also includes an analysis of spatio-temporal variability of power generation, the sensitivity study of feed-in profiles and some statistical analysis.

3.1. Validation

Validation of model results is an essential step towards producing any high quality database. The time-series of PV, CSP, wind and hydro power for different countries is validated depending on the availability of the measurement data. Our results are also compared with simulations from other working groups in related fields. Apart from time-series validation, resource distributions are compared with available maps for different countries as well as for Europe. Our approach of retrieving irradiance from satellites is well validated in literature [12] and is also compared with other existing methodologies [7]. For wind, the validation is further extended to compare statistically downscaled wind speed with dynamically downscaled wind speeds from a WRF (Weather Research Forecast) simulation.

3.1.1. Validation of PV feed-in

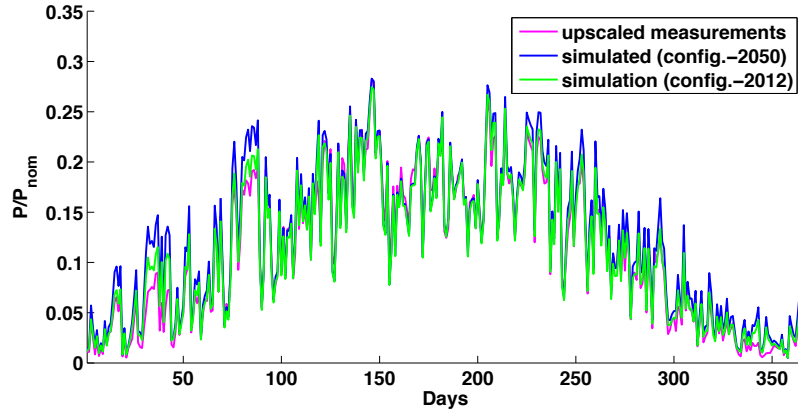


Figure 11: Validation of normalised daily PV feedin with measurements for Germany, 2012

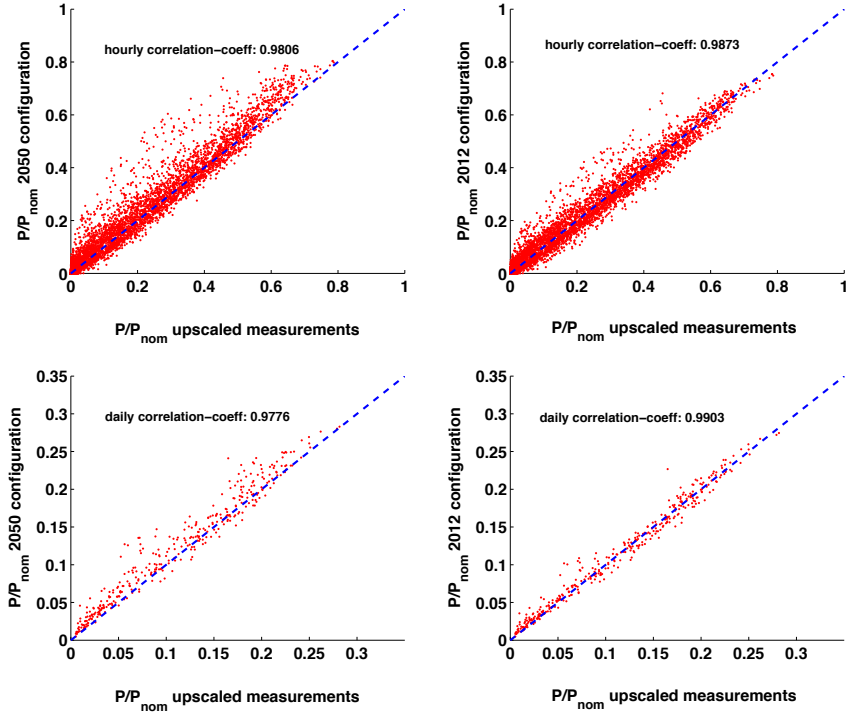


Figure 12: Hourly (top) and daily (bottom) comparison of PV simulations using 2050 (left) and 2012 (right) module configurations with upscaled measurements for Germany, 2012

	Upscaled measurements	Simulation: 2012 config.	Simulation: 2050 config.
Gross production (TWh)	27.9	68.5	74.0
Installed capacity (GW)	25-32	69	69
Capacity factor	0.111	0.113	0.122
Standard deviation of normalised power	0.170	0.169	0.183

Table 4: Overview of results from hourly PV time-series of 2012 for Germany

		Measurement - Simulation-2012	Measurement - Simulation-2050
Correlation coefficient	hourly	0.987	0.981
	daily	0.990	0.987
Relative RMSE	hourly	0.244	0.350
	daily	0.091	0.168

Table 5: Comparison between normalised PV power with 2012 and 2050 module configurations using upscaled measurements for Germany, 2012

Most European countries do not provide adequate information on PV power feed-in. For Germany, however, four transmission system operators (TSOs) provide PV power feed-in data from all over the country (Fig. 3). The data on the actual PV feed-in within each control zone of Germany is based on the projection of the feed-in measurements from a limited number of reference PV power plants. Hence, here onwards, the PV feed-in data collected from all these TSOs and aggregated to the country level will be referred to as ‘upscaled measurement’. The quarter-hourly data from the TSOs is averaged to hourly values rounding around the hours for better comparison with the model results.

This section includes the discussion of the comparison of country level PV feed-in time-series from our model with the ‘upscaled measurement’ data from TSO for 2012. However, these two time-series have very different installed capacities, so they are normalised to their respective capacities to allow reasonable comparison. Since detailed information on the gradual changes in PV capacity throughout the year 2012 is unknown, a linear increase in capacity is assumed from $\sim 25\text{GW}$ in the beginning of 2012 to $\sim 32\text{GW}$ by the end of 2012 [1].

It is to be noted that not all PV systems in the real world today are configured optimally. However, our model uses optimal module configurations from the ISI meta-study [17] to address issues of 2050. Hence, to better compare the PV feed-in with ‘upscaled measurement’ of 2012, it is recalculated using module configurations of Germany in recent time.

The comparison of PV feed-in from our model for Germany with the ‘upscaled measurement’ time-series from the TSOs indicate good agreement (Fig. 11). Our results not only reproduces similar patterns over the annual course, but also captures the daily fluctuations to a good extent. Fig. 11 and 12 show the improvements achieved by simulating with 2012 configuration over the original time-series computed with the optimal module configurations for 2050. The differences are most prominent for Autumn and Spring seasons because the PV power output is strongly influenced by the rapidly changing solar elevations during these months. A quantitative measure of how well our simulated PV feed-in matches the ‘upscaled measurements’ is summarised in Table 4

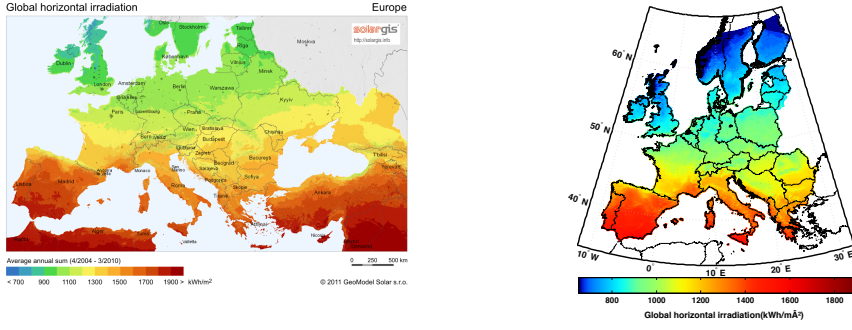


Figure 13: European map of average annual sum (April, 2004 - March, 2010) of global horizontal irradiance from SolarGIS (left) (SolarGIS©2011 GeoModel Solar) and our simulation (right)

and 5. While Fig. 11 compares daily PV feed-in time-series from simulation and measurements, Fig. 12 shows their correlation at different temporal resolutions (hourly and daily). PV simulation with 2012 configuration shows reduction in dispersion on both hourly and daily scales of Fig. 12 compared to the time-series with 2050 configuration.

We have also qualitatively compared the irradiance distribution from other existing studies. Fig. 13 compares average annual GHI map for Europe from our simulation with the one from SolarGIS. SolarGIS is a geographical information system that integrates solar resource and meteorological data for planning and performance monitoring of solar energy systems. Similarly, Fig. 14 compares average annual irradiance on inclined planes from our simulations with the PVGIS map of Europe. PVGIS is another geographical information system that provides climate data for the performance assessment of photovoltaic (PV) technology in Europe. The existing differences in the irradiance maps from our simulations and that from SolarGIS or PVGIS can result from using different models that apply different resolutions, different parameterizations and different sources of input data. Overall we find that our results are in good agreement with the existing studies.

3.1.2. Validation of CSP feed-in

For CSP technology, very limited information is available from the power plants in Europe. Thus it is not possible to compare country-level time-series of CSP, as we did for solar PV. The direct normal irradiance (DNI), which is of particular relevance to concentrated solar technologies, follow a linear relationship with power output from